Biomedicine & Pharmacotherapy 109 (2019) 1462–1477

Contents lists available at ScienceDirect

Biomedicine & Pharmacotherapy

journal homepage: www.elsevier.com/locate/biopha

Piperlongumine, a piper alkaloid targets Ras/PI3K/Akt/mTOR signaling axis to inhibit tumor cell growth and proliferation in DMH/DSS induced experimental colon cancer

Sandeep Kumar, Navneet Agnihotri*

Department of Biochemistry Basic Medical Science Block-II Sector-25, South Campus, Panjab University, Chandigarh 160014, India

ARTICLE INFO

Keywords:
Piperlongumine
Colorectal cancer
Apoptosis
Cell proliferation
PI3K/Akt/mTOR signaling pathway

ABSTRACT

Colorectal cancer (CRC) is the most common carcinoma of the digestive tract. The slow growing nature of CRC offers a great opportunity for prevention strategies. The concept of chemoprevention of colorectal cancer using plant derived natural products is gaining substantial attention because it is an inherently safe and cost-effective alternative to conventional cancer therapies. Piperlongumine (PL), a natural alkaloid present in *Piper longum* Linn has been reported to exhibit notable anticancer effects in various *in vitro* studies. Nonetheless, the chemopreventive potential of PL has not been studied in experimentally induced colon cancer yet. Ras/PI3K/Akt/mTOR signaling axis plays a central role in promoting tumor cell growth, proliferation and survival by inhibiting apoptosis. In the present study, we demonstrated, *for the first time,* the chemopreventive effects of PL in DMH + DSS induced colon carcinogenesis animal model. We showed that PL displayed potent antineoplastic activity against colon cancer cell growth by targeting Ras proteins and PI3K/Akt signaling cascade. PL mediated inhibition of tumor cell growth was associated with inhibition of Ras protein levels and its preferred companion protein PI3K levels that led to suppressed activity of Akt/NF-κB, c-Myc and cyclin D1. It was also found that PL arrested the cell cycle progression at G2/M phase and induced mitochondrial apoptotic pathway by down-regulating Bcl-2 levels. Furthermore, the results of liver and kidney toxicity suggested that PL exhibit no toxicity in animals. Our results suggest that PL may be an effective chemopreventive agent for colon cancer.

1. Introduction

Colorectal cancer (CRC) is one of the most commonly diagnosed carcinomas worldwide. The global burden of CRC is expected to increase by 60% with more than 2.2 million new cases and 1.1 million deaths by 2030 [1]. Currently surgery, chemotherapy and radiotherapy are prevailing strategies to treat CRC. Among these, surgery is useful only when CRC is diagnosed at early stages. However, for malignant cancer, chemotherapy and radiotherapy are advised that cause severe side effects and deteriorate the quality of life of patient [2]. For example, 5-fluorouracil, a common chemotherapeutic agent causes myelotoxicity, cardiotoxicity and vasospastic in few documented cases [3]. On the other hand, cancer chemoprevention deals with consumption of natural products or bioactive compounds from mother nature to combat the development of cancer [4]. As these products are pharmacologically safe and exhibit no side effects, thus provide an alternative to the use of conventional chemotherapeutic drugs. Epidemiological and pre-clinical data suggest that various natural compounds and dietary elements possess chemopreventive properties by modulating multiple pathways such as apoptosis and cell cycle regulation which are normally disturbed in tumor initiation, promotion and progression. In addition, natural compounds have been shown to enhance the host immune system and sensitize malignant cells to cytotoxic agents [5]. With the advent of high-throughput screening technologies, a myriad of plant products have been discovered that have shown very promising anticancer properties *in vitro* but are yet to be evaluated in animal models and humans [6]. Therefore, it is imperative to evaluate anticancer activity using appropriate animal model. The animal models provide important tools for deciphering the mechanism of CRC pathophysiology so that focused human clinical trials related to chemotherapy can be conducted with greater chances of success. In that regard, many murine models of sporadic and inflammation related CRC have been developed including chemically induced CRC, genetically engineered mouse models and xenograft models. Among the chemically induced CRC models, a combination of single intraperitoneal 1,2-dimethylhydrazine (DMH) with one week exposure to inflammatory agent dextran sulphate

* Corresponding author.
E-mail addresses: sandeepmahiwal40@gmail.com (S. Kumar), navneet_agnihotri@pu.ac.in (N. Agnihotri).

https://doi.org/10.1016/j.biopha.2018.10.182
Received 25 June 2018; Received in revised form 29 October 2018; Accepted 31 October 2018

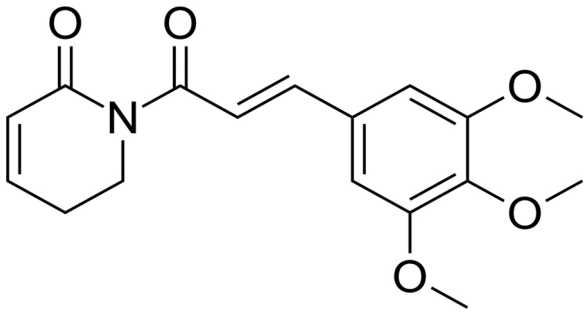

Fig. 1. Chemical structure of piperlongumine (PL).

sodium (DSS) in mice dramatically shortens the latency time for CRC development as well as mimics aberrant crypt foci–adenoma–carcinoma sequence of human CRC [7,8]. Because of its high reproducibility, potency and affordability, DMH + DSS induced CRC model has become an outstanding platform to study the key molecular events of colon carcinogenesis for evaluation of chemopreventive interventions.

Spices have been traditionally used for their flavor enhancement characteristics in Indian cuisine and are a rich source of phytochemicals that suppress the process of carcinogenesis. Many potent anticancer compounds such as curcumin (Turmeric), zingerone (Ginger), allicin, diallyl sulphide, diallyl disulphide and diallyl trisulphide (Garlic) have been isolated from common dietary spices [9]. Piperlongumine (PL, piplartine, 5,6-dihydro-1-[(2E)-1-oxo-3-(3,4,5-trimethoxyphenyl)-2-propenyl]-2(1H)-pyridinone) (Fig. 1) is a biologically active alkaloid isolated from common Indian dietary spice *Piper longum* Linn commonly called Long pepper. PL was identified to kill cancer cells selectively both *in vitro* and *in vivo* without affecting the normal cells [10]. PL has been reported to exhibit cytotoxic activity against various cancer cell lines and inhibit tumor size in mouse xenograft models *via* multiple cellular processes including accumulation of reactive oxygen species (ROS) [10], activation of C/EBP homologous protein (CHOP) [11], suppression of LMP-1 (EBV-encoded oncogene) expression [12], activation of AMPK phosphorylation [13], inhibition of NF-κB [14,15] activation of ERK [16], promotion of autophagy [17–19], induction of GADD45α and inhibition of telomerase reverse transcriptase activity [20]. Recently, PL has been reported to inhibit PI3K/Akt/mTOR pathway in lung [21] and triple negative breast cancer cell lines [22]. However, till date, there has been no report regarding the effect of PL in colon carcinogenesis.

Therefore, the present study was designed to evaluate the chemopreventive potential of PL and its mechanism of action in DMH/DSS induced experimental colon carcinogenesis.

2. Materials and methods

2.1. Chemicals

Piperlongumine (PL) was purchased from Indofine Chemical Company (Hillsborough, NJ, USA). The purity of the compound was more than 98% as per datasheet provided by the manufacturer. Ethylenediaminetetraacetic acid (EDTA), 1,2 –Dimethylhydrazine (DMH), dimethylsulfoxide (DMSO), phenylmethylsulfonyl fluoride (PMSF), dithithreitol (DTT), Hoechst 33342 and propidium iodide (PI) dye were received from Sigma chemical company (St. Louis, MO, USA). Dextran sulphate sodium salt (DSS) was purchased from MP Biomedicals (Solon, OH, USA). Monoclonal antibodies against β-actin, cleaved caspase-3, NF-κB p65 subunit, PI3 Kinase p85, phospho-Akt (Ser 473) and Akt were purchased from Cell Signalling Technology (Beverly, MA, USA). Primary antibodies against Bax, Bcl-2, pan-Ras, MEK 1/2, p-MEK 1/2 (Ser 218/Ser 222), Cyclin D1, c-Myc and PARP1/2 were procured from Santa Cruz Biotechnology (Minneapolis,MN, USA). Primary antibody against phospho-ERK 1/2 (T202/Y204) was purchased from BD Bioscience (Franklin Lakes, NJ, USA). Clarity™ ECL Western Blotting Substrate was purchased from Bio-Rad (Hercules, CA, USA). Annexin V/PI assay kit for quantification of apoptosis was procured from BD Biosciences (San Jose, CA, USA).

2.2. Experimental animals

Five to six week old male Balb/c weighing 20–25 g were procured from Central Animal House, Panjab University, Chandigarh, India. All experimental protocols were first approved by Institutional Ethics Committee (PU/IAEC/S/14/47) and conducted according to the guidelines of Indian National Science Academy for the use and care of experimental animals. The animals were housed in ventilated polypropylene cages and acclimatized for one week in the animal room before the commencement of the study. The animals were fed on standard mouse chow pellet diet supplied by Aashirwad industries, Punjab, India and water *ad libitum*.

2.3. Experimental design

Male Balb/c mice (N = **40**) were divided equally into five groups. All doses including DMH, PL and their vehicles were given intraperitoneally.

2.3.1. Control group

The animals of this group received a single dose of 1 mM EDTA, pH = 6.5 (vehicle for DMH).

2.3.2. DMSO only

These animals were administered with 10% DMSO corresponding to the amount utilized for PL (vehicle for PL) daily for 10 weeks.

2.3.3. DMH + DSS group

The animals of this group were given a single dose of DMH (20 mg/kg b.w.). One week after DMH exposure, DSS (3%) was given in drinking water for one week, followed by normal drinking water for next two weeks. The animals were subjected to three such alternate cycles of DSS.

2.3.4. DMH + DSS + PL group

The animals of this group were treated with PL (3.6 mg/kg b.w.) daily for a period of two weeks prior to the exposure of DMH and DSS as mentioned in group 3 and continued till the last DSS cycle. The criteria for selection of dosage of PL are given in supplementary data (Supplementary Tables 1 and 2).

2.3.5. PL only group

The animals of this group were administered PL (3.6 mg/kg b.w.) daily for a period of 10 weeks.

The animals were kept for a total period of 20 weeks and sacrificed subsequently by cervical dislocation.

2.4. Body weight gain and food intake

Body weight was measured on weekly basis and gain in average body weight for each group was calculated from the initial weight subtracted from final weight during the treatment period. Food intake was also monitored on daily basis and analyzed on weekly basis.

2.5. Tumor burden and volume

The colon was excised and washed with cold PBS. The distended and everted colonic mucosa was evaluated grossly as well as with methylene blue staining for determining tumor burden and tumor volume. Number of tumor nodules per animals was designated as tumor burden. Two dimensional measurements of each tumor nodule were

done with digital Vernier caliper (Cen Tech, Camarillo, CA, USA).The tumor volume was calculated according to the formula given below.

Tumor volume (mm^3) = length (mm) x [width (mm)]^2/2

The tumors were further classified as large (> 20 mm^3), medium (10-20 mm^3) and small (1-10 mm^3) and smallest (1 mm^3 or less).

2.6. Histopathology

The colon was removed and flushed with cold PBS and distal end (2–3 cm) was fixed in 10% neutral buffered formalin. Sections of 4–5 μm thickness were prepared and stained with standard hematoxylin and eosin staining method. The slides were photomicrographed using Nikon Eclipse 80i microscope and evaluated for the presence of adenoma, hyperplasia and cancer *in situ* by a trained and qualified histopathologist.

2.7. Isolation of colonocytes

The colonocytes were isolated by the method of Sanders *et al* with slight modifications [23]. The entire colon was cut longitudinally to expose lumen and placed in warm Ca^{2+} and Mg^{2+} free Hank's buffered salt solution (HBSS) containing 30 mM EDTA, 5 mM DTT and 0.1% BSA. After 15 min shaking incubation at 37 °C, the colon was transferred into warm HBSS containing 1.3 mM$CaCl_2$, 1 mM $MgSO_4$, 0.5% BSA and dispase (1.2 mg/ml) for 30 min. The mucosal side of the colon was then gently scraped and the cellular suspension was filtered through a nylon filter (70 μm) to obtain single cell suspension. The isolated colonocytes were then centrifuged at 2000 rpm for 10 min and counted using hemocytometer (Marienfeld, LK, Germany). Trypan blue exclusion method [24] was used to assess the viability of isolated colonocytes and cells with viability index of 85–90% were taken for further experimentations.

2.8. Analysis of cell cycle progression

The percentages of isolated colonocytes in the Go/G1, S and G2/M phases of cell cycle were quantified on flow cytometer using Cycletest Plus DNA reagent kit (BD Biosciences, San Jose, USA). Briefly, the isolated colonocytes were fixed in70% ice cold ethanol dropwise with constant shaking. The cells were treated with RNase A (200 μg/ml) solution for 30 min and then with PI (10 μg/ml) for 10 min at room temperature. The samples were acquired on flowcytometer (BD FACSCalibur, San Jose, USA) and a total of 5000 events were taken for cell cycle analysis. The fluorescence histograms of propidium iodide (PI) stained nuclei were analyzed by FCS Express V3 software to determine the percentage of cells in different phases.

2.9. Measurement of Apoptotic index

Apoptotic index in different animal groups was assessed by the following methods:

2.9.1. Annexin V/PI apoptosis assay

The percentage of apoptotic cells was quantitatively determined using FITC Annexin V Apoptosis Detection Kit (BD Biosciences, San Jose, USA) as per the protocol mentioned by the manufacturer. Briefly, approximately 2×10^7 isolated live colonocytes were stained with FITC labeled Annexin V and propidium iodide (PI) for 15 min at room temperature in the dark. After appropriate washing, the acquisition from each sample was conducted on BDFACS Canto Flow Cytometer (BD Biosciences, San Jose, USA) and the collected data were analyzed using the BDFACS Diva software. The important controls (*i.e.* unstained cells, cells stained with FITC Annexin V alone and PI alone) were also run simultaneously. The untreated cell population was used to define the basal level of apoptotic and dead cells. The percentage of apoptotic cells was then determined by subtracting the percentage of apoptotic cells in the untreated population from the percentage of apoptotic cells in the treated population.

2.9.2. Hoechst 33342/PI staining methods

The percentage of live and apoptotic cells was estimated by Hoechst 33342/PI staining method. Freshly isolated colonocytes ($1–2 \times 10^6$) were stained with 10 μl of Hoechst 33342 dye (H33342, 1 mM) at 37 °C for 1 h. After washing, the cells were subsequently incubated with 10 μl of PI (1 mg/ml) at 37 °C for 10 min. Photomicrographs (four random fields from each slide) were acquired using the fluorescent microscope (Nikon Eclipse 80i) and analyzed using Northern Eclipse imaging Elements-D (NIS-D) software. Photomicrographs of cells with H33342 and PI were merged. In merged photomicrographs, cells with pink color represent apoptotic cells whereas faint blue were considered to be normal cells. The cells with red fluorescence represent necrotic/dead cells.

2.10. Western blotting

Distal end of colon tissue was homogenized in ice cold lysis buffer [50 mM Tris − HCl (pH 7.4), 1% Triton-X, 2 mM DTT, 1 mM PMSF, 0.1% sodium dodecyl sulfate (SDS), 100 mM sodium chloride (NaCl), 5 mM EDTA, and 0.2% EZBlock™ Universal Protease and Phosphatase Inhibitor Cocktail (BioVision, Inc.Milpitas, CA, USA). A total of 75 μg protein of tissue lysate from each animal group was electro-transferred to polyvinylidenedifluoride membranes (Bio-Rad, Hercules, USA). After blocking with 3% BSA, the membranes were incubated with primary antibodies for Cleaved caspase-3 (1:1000), PARP1/2 (1:1000), Bax (1:1000), Bcl-2 (1:1000), c-Myc (1:1000), Cyclin D1 (1:1000), pan-Ras (1:1000), phospho-MEK 1/2 (1:300), MEK 1/2 (1:1000), Phospho-ERK 1/2 (1:1000), Phospho-Akt (Ser 473, 1:3000), Akt (1:2000), PI3 Kinase (1:3000), NF-κB p65 (1:1000) and β-actin (1:5000) overnight at 4 °C. The membranes were then washed with Tris - buffered saline (TBS) containing 0.1% Tween-20 and incubated with corresponding horse radish peroxidase (HRP)-labelled goat anti-mouse IgG (1:3000) and anti-rabbit-IgG (1:5000) at room temperature for 1 h. The immunoblots were developed with Enhanced Chemiluminescence Detection Kit (Bio-Rad, Hercules, USA) and visualized on FluorChem M (ProteinSimple, San Jose, USA). Densitometry analysis was performed with AlphaView software provided with the instrument.

2.11. Liver and kidney toxicity parameters

To assess the liver and kidney toxicity caused either by carcinogen exposure or PL administration, fresh blood was collected into the glass tubes by penetrating the retro-orbital sinus in mice with a capillary tube and placed in slanting position for 1 h. The clotted blood was centrifuged at 2000 g for 15 min. The clear serum was used for the estimation of serum glutamate oxaloacetate transaminase (SGOT, AST), serum glutamate pyruvate transaminase (SGPT, ALT), blood urea nitrogen (BUN) and creatinine by using commercially available kits (Reckon Diagnostics Pvt. Ltd Baroda, India).

2.12. Statistical analysis

The results are expressed as mean ± standard deviation (SD). The differences between the groups were assessed by one-way analysis of variance (ANOVA) using GraphPad Prism 5 software package for Windows. Post hoc test Tukey was performed for intergroup comparisons using the least significant difference (LSD). A value of $p < 0.05$ was considered to indicate a significant difference between groups.

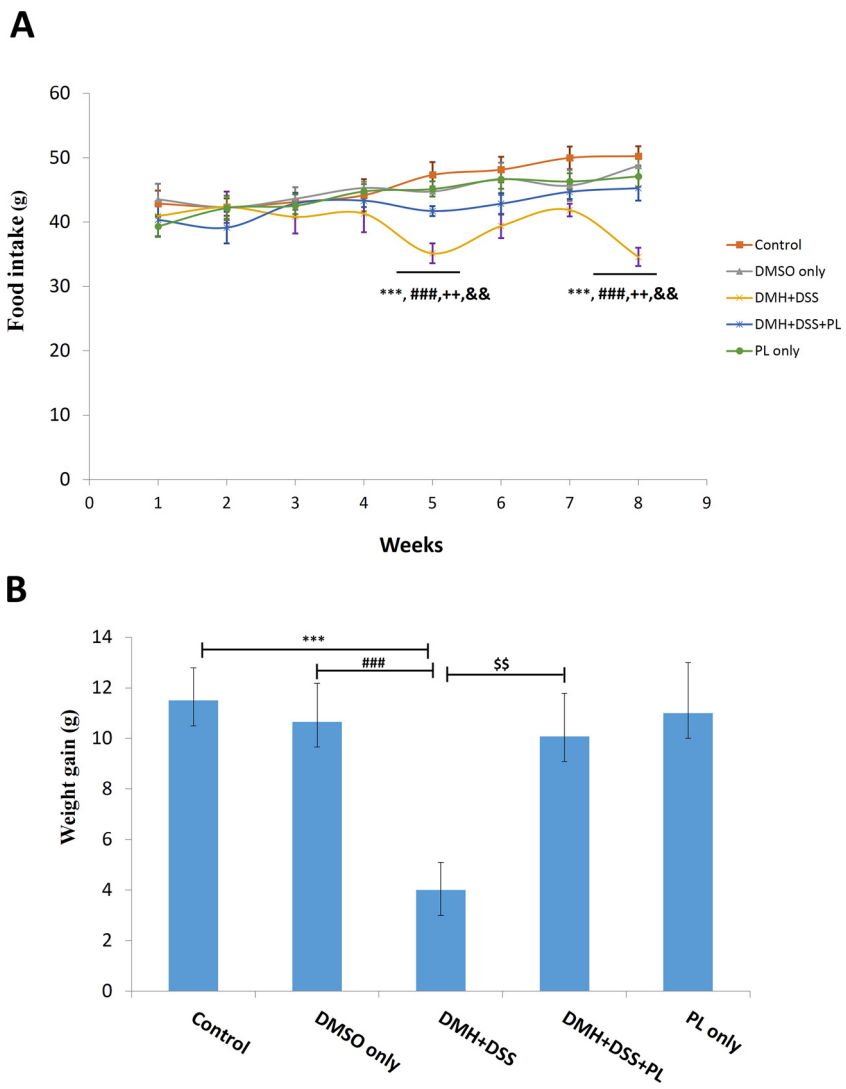

Fig. 2. Effect of PL administration on **A)** daily food intake and **B)** gain in body weight. Values are expressed as mean ± SD (n = 5). $^{***}p < 0.001$ w.r.t. Control group, $^{###}p < 0.001$ w.r.t. DMSO group, $^{\$\$}p < 0.01$ w.r.t. DMH + DSS group. $^{++}p < 0.01$ w.r.t. DMH + DSS + PL group. $^{\&\&}p < 0.01$ w.r.t. PL group.

3. Results

3.1. Effect of PL on body weight gain and food intake

Average food intake and gain in body weight were recorded on weekly basis and the results are expressed in Fig. 2 A and B. The animals in the control and corresponding vehicle treated groups exhibited an increase in food intake and gain in average body weight throughout the treatment tenure and were not significantly different from each other. On the other hand, food consumption in mice treated with DMH + DSS was significantly decreased with a concomitant reduction in gain in average body weight. However, animals treated with DMH + DSS + PL showed a significant improvement in food intake and gain in average body weight as compared to DMH + DSS treated animals.

3.2. Effect of PL on colon morphology, tumor burden and volume

The potential of PL on tumor growth inhibition was assessed through gross examination of normal and methylene blue stained colon, determination of tumor burden/animal and volume (Fig. 3). The colon of control animals, DMSO only and PL only treated animals had normal colon with no sign of injury (Fig. 3 A & B (a,b,e). In contrast, colon excised from DMH + DSS group animals exhibited a high number of visible tumor nodules of different sizes such as large, medium, small and smallest (Fig. 3 C). Treatment with PL to DMH + DSS treated animals led to a significant reduction not only in tumor burden but also in tumor size.

3.3. Effect of PL on histopathological features of colon

Histopathological evaluation revealed that the colon of mice from control, DMSO only and PL treated groups had normal histoarchitecture with no signs of apparent abnormality (Fig. 4). In contrast, high order of irregular crypts, loss of goblet cells and inflammation rich areas were observed in DMH/DSS group. In addition, there was evident malignant transformation in the colon with features of polyploid adenoma, hyperplasia and cancer *in situ* in these animals (Fig. 4). However, PL administration in DMH + DSS treated animals not only maintained the normal crypt architecture and restoration of goblet cell population but also abrogated the formation of adenoma and infiltration of inflammatory cells (Fig. 4).

3.4. Effect of PL on cell cycle progression

In order to understand the mechanism of PL mediated tumor growth

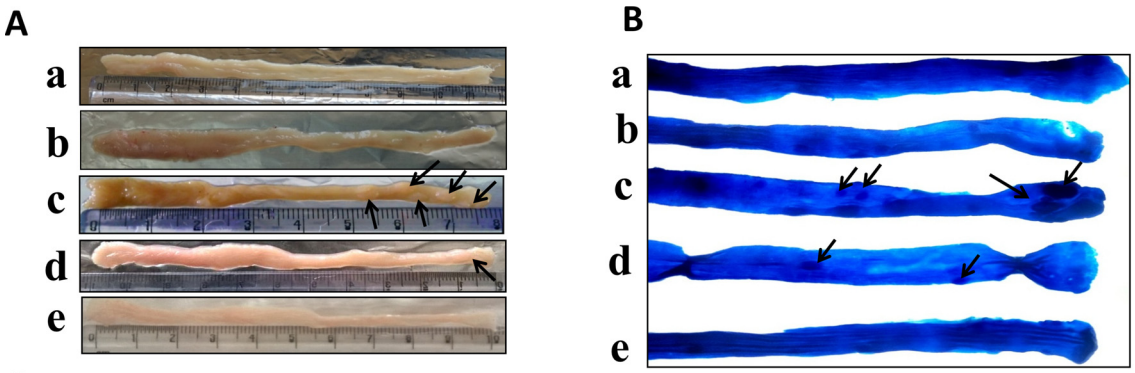

C

Groups	Tumor burden (no. of nodule/ animals)	Tumor volume (mm^3)			
		Large (> 20 mm^3)	Medium (10-20 mm^3)	Small (1-10 mm^3)	Smallest (≤1 mm^3)
Control	0	0	0	0	0
DMSO only	0	0	0	0	0
DMH+DSS	7.25±1.25$^{*,\#}$	27.56±1.46$^{*,\#}$	13.49±3.28$^{*,\#}$	4.44±1.04$^{*,\#}$	0.67±0.15$^{*,\#}$
DMH+DSS+PL	1.66±0.57$^{*,\#,\&}$	0	0	7.36±1.32$^{*,\#,\&}$	0
PL only	0	0	0	0	0

Fig. 3. Antitumor effect of PL. **A)** Gross examination of mouse colon showing visible tumor nodules (arrow head) **B)** Representative images of methylene blue stained whole mount colon segments. a: control group, b: DMSO only group, c: DMH + DSS group, d: DMH + DSS + PL group and e: PL only group). **C)** Represents the tumor burden and volume determined using vernier caliper. Values are expressed as mean ± SD (n = 5). $^{*}p < 0.001$ w.r.t. control group, $^{\#}p < 0.001$ w.r.t. DMSO only group, $^{\&}p < 0.01$ w.r.t. DMH + DSS group (For interpretation of the references to colour in this figure legend, the reader is referred to the web version of this article).

inhibition, cell cycle analysis was done in colonocytes isolated from different groups and the results are depicted in Fig. 5. On treatment with DMH + DSS there was a significant increase in the percentage of cells in S phase and G2/M phase indicating a high cell division rate in these animals as compared to control animals. On the other hand, cell cycle analysis of colonocytes from DMH + DSS + PL group animals showed a significant increase in the percentage of cells in G2/M phase as compared to DMH + DSS group suggesting a growth arrest.

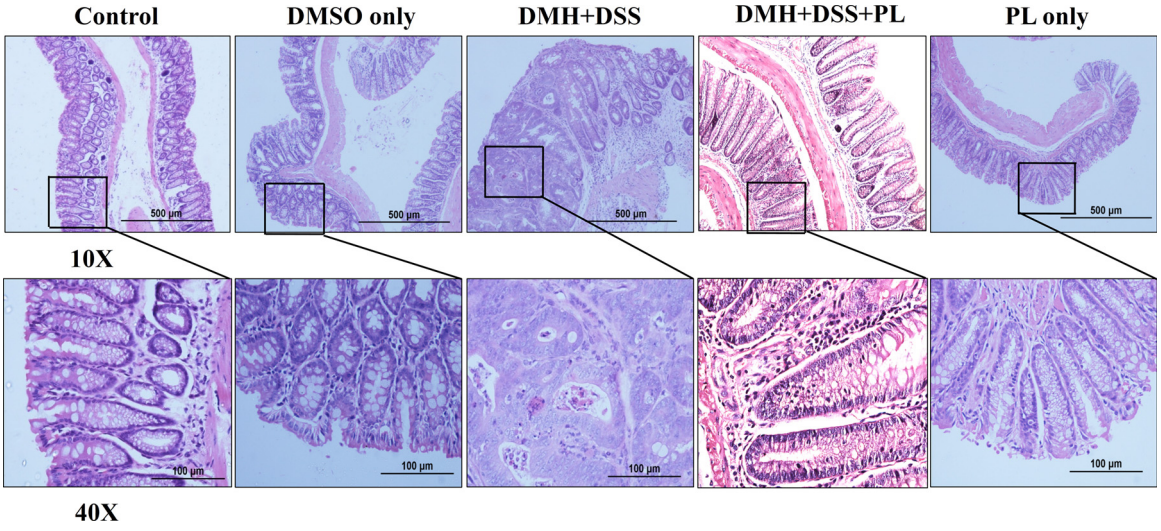

Fig. 4. Representative images of H&E stained colon sections from different groups. Control group showing the normal colon architecture and crypt morphology, DMSO only group showing no major alteration in colon histological features as compared to control group, DMH/DSS group depicting complete loss of goblet cells, crypt architecture and development of adenoma carcinoma, DMH/DSS/PL group showing less perturbed crypts and improved population of goblet cells in most of colon sections. PL only group showing normal crypt structure and goblet cell distribution. Each image is a representative of four randomly selected fields (magnification: 10×, scale bar represents 500 µm in upper row and inset magnification: 40× and scale bar 100 µm).

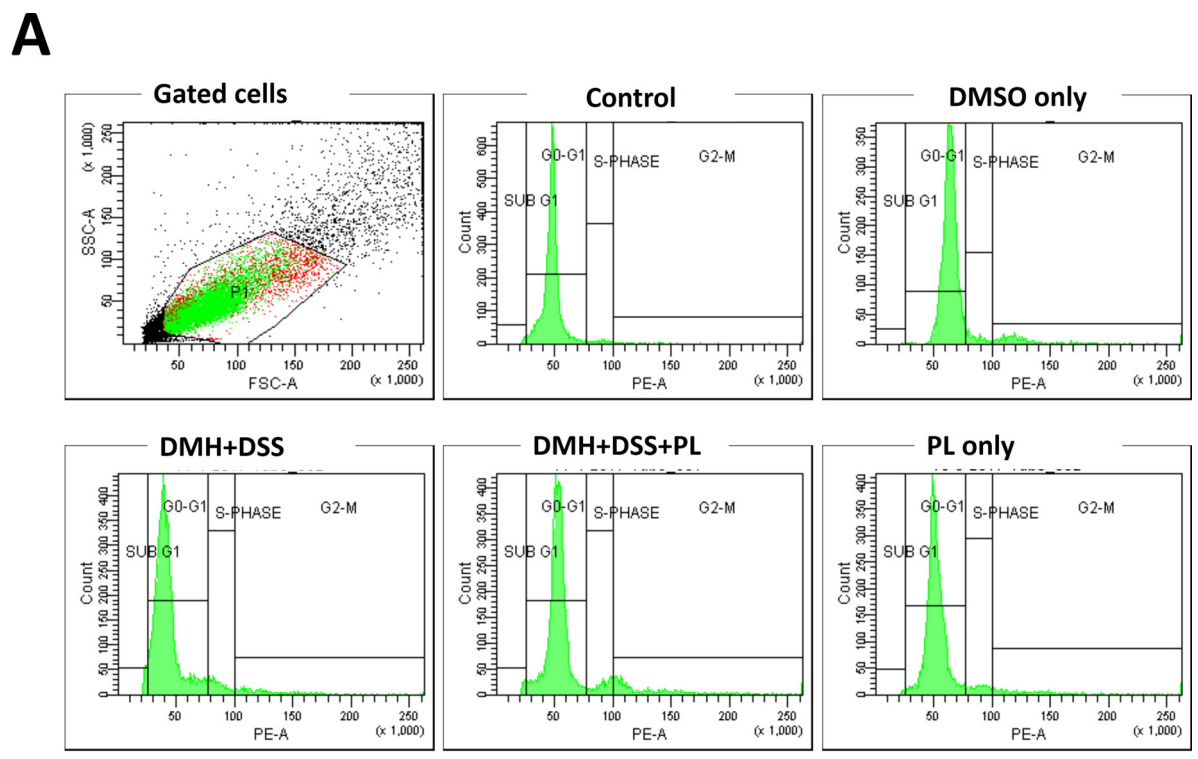

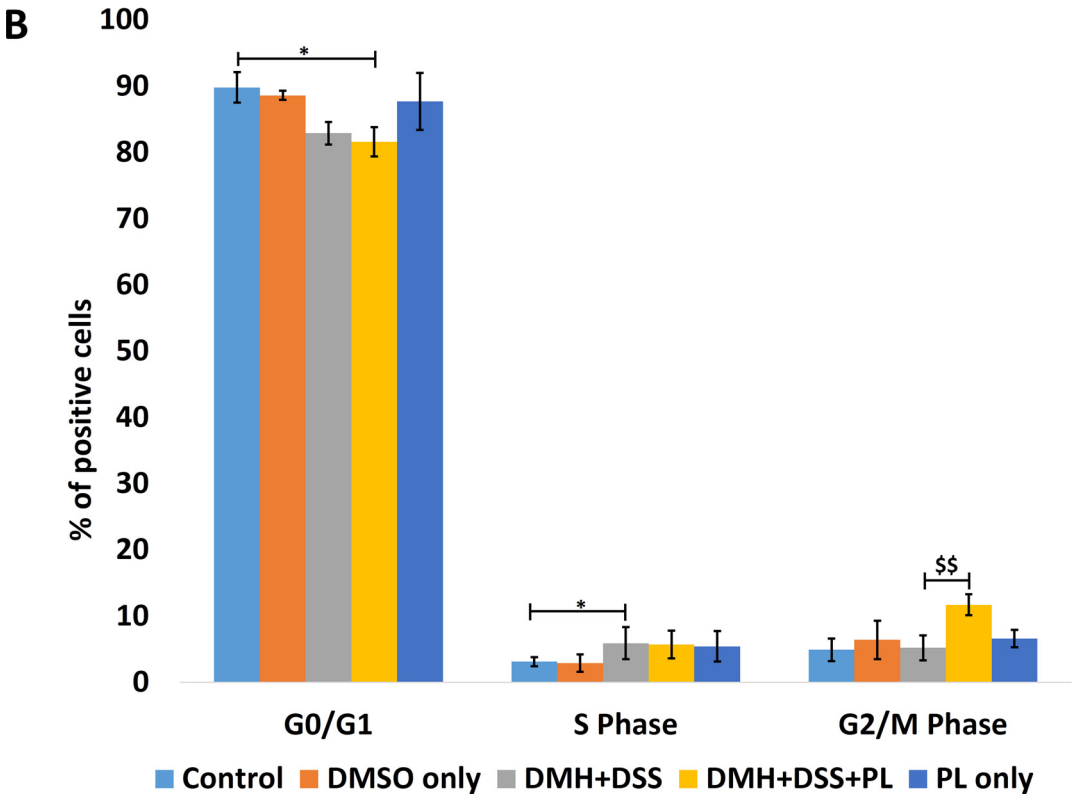

Fig. 5. Effect of PL on cell cycle progression in isolated colonocytes in various groups. **A)** Representative histograms showing percentage % of cells in Go/G1, S and G2/M phase from different groups. A Gated cells represent population of colonocytes selected for cell cycle analysis. **B)** Flow cytometric analysis of cell cycle distribution.The values are expressed as mean ± SD for n = 5 animals. *$p < 0.05$ w.r.t. control, $^{\$\$}p < 0.01$ w.r.t. DMH + DSS.

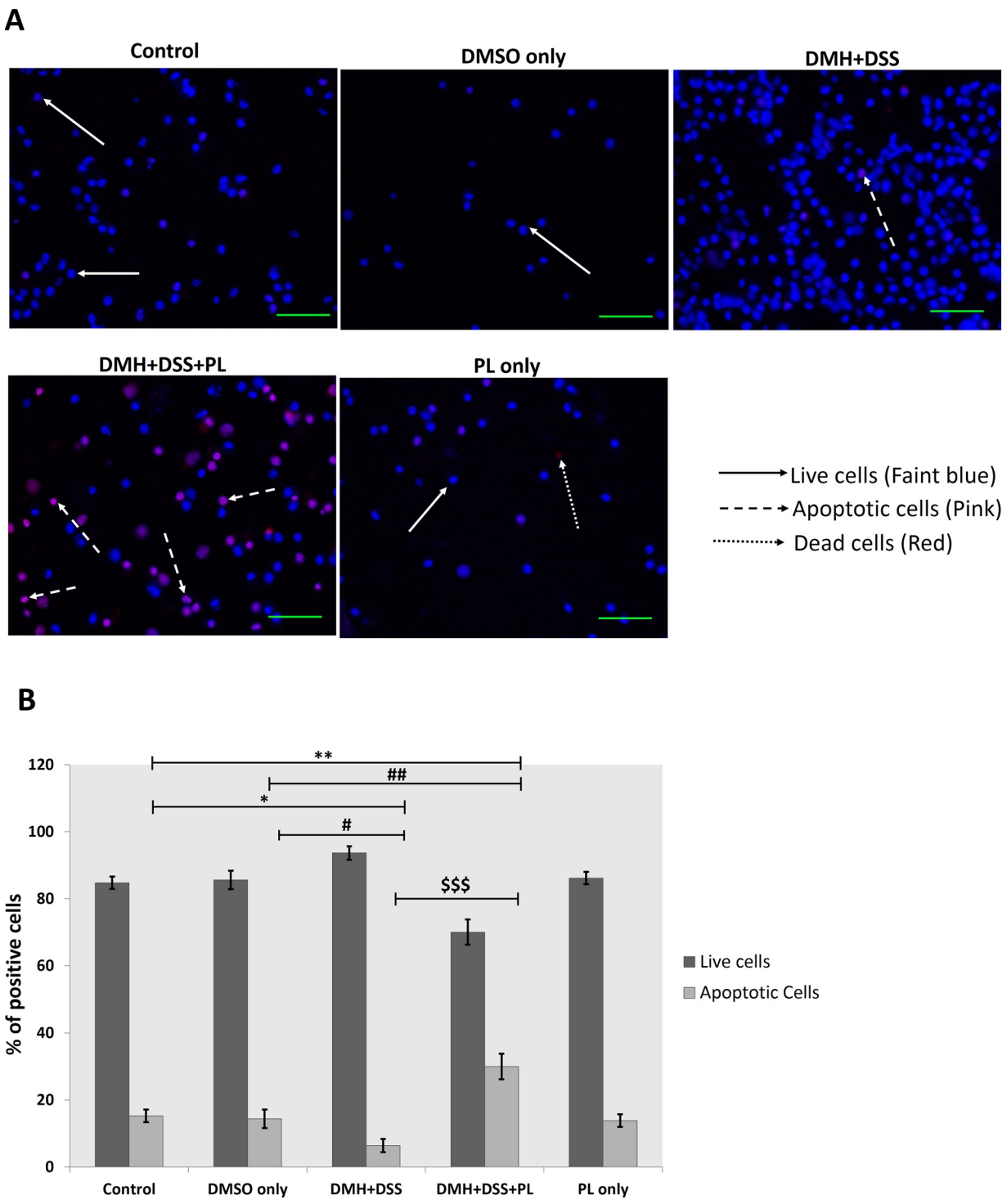

Fig. 6. Effect of PL on apoptotic index using Hoechst (33342) and propidium iodide staining method. **A)** Representative images showing fluorescence of isolated colonocytes stained with Hoechst (H33342) and propidium iodide in various groups. Here blue fluorescence represents live cells, pink fluorescence denotes apoptotic cells and red represents the dead cells. Images were taken at magnification of 40X and scale bar represents 50 µm. **B)** Graphical representation of per cent apoptotic cells in different groups. The values are expressed mean ± SD of n = 5 observartion from each group. *p < 0.05, **p < 0.01 w.r.t. control, $^{\#}$p < 0.05, $^{\#\#}$p < 0.01 w.r.t. DMSO only and $^{\$\$\$}$p < 0.001 w.r.t. DMH + DSS group (For interpretation of the references to colour in this figure legend, the reader is referred to the web version of this article).

However, there was no significant change in the percentage of cells in different phases of cell cycle in any of the control groups.

3.5. Effect of PL on apoptosis

The fact that cell cycle arrest at G2/M phase leads to significant apoptosis has been documented in several cancer cell lines [25]. Therefore we further evaluated the effect of PL on apoptosis by Hoechst 33342/PI staining and Annexin V/PI assay (Figs. 6 and 7). The cells isolated from control, DMSO only and PL only treated animals exhibited a normal apoptotic index. DMH + DSS treatment to animals resulted in a significant inhibition in apoptotic index as compared to control

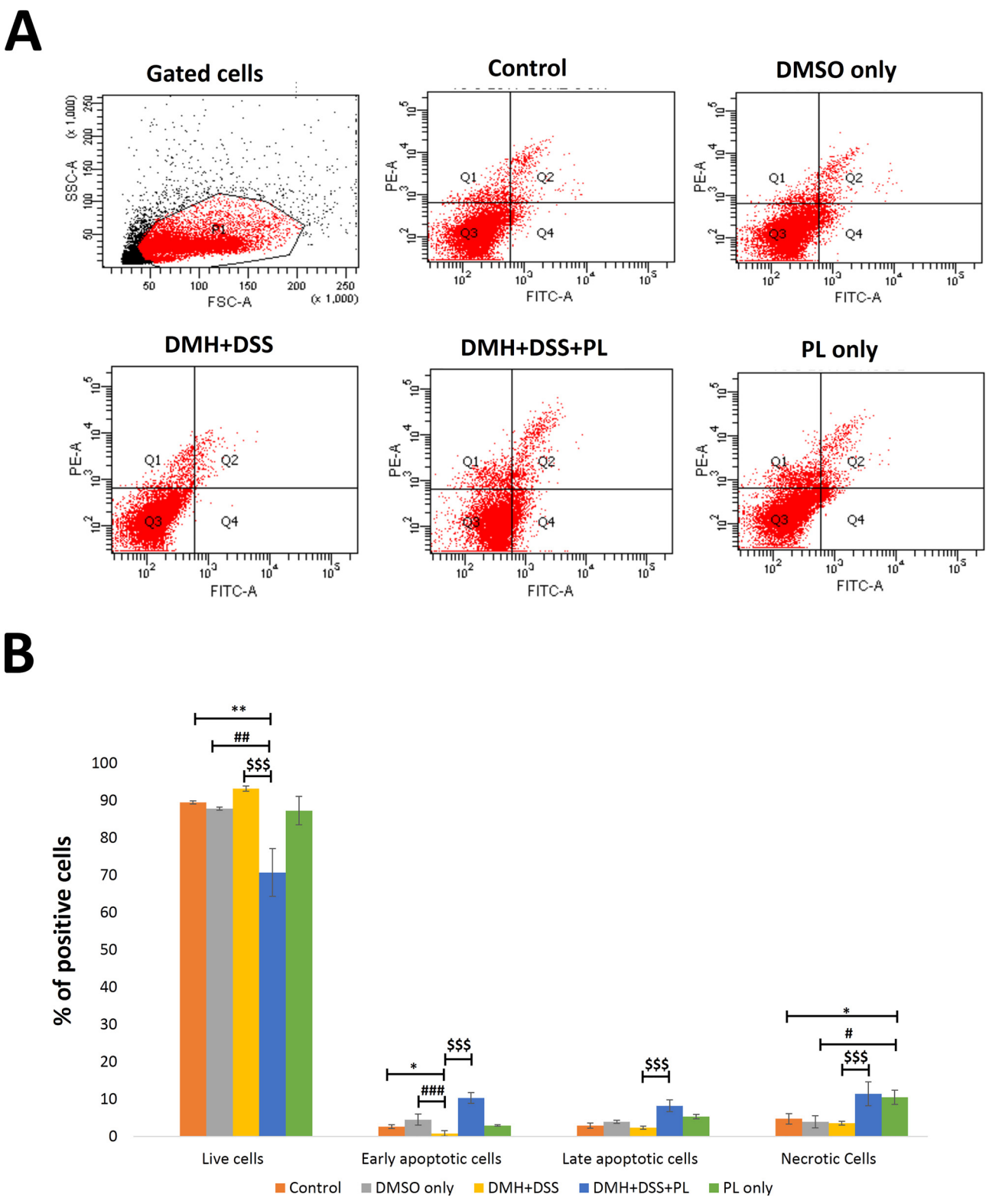

Fig. 7. Effect of PL on apoptotic index using Annexin V and propidium iodide assay. **A)** Representative photograph showing percentage of live, early, late and necrotic cells using Annexin–PI staining by flow cytometric method in different groups. Gated cells represent population of colonocytes selected to assess apoptosis. Q1 quadrant represents the percentage of necrotic cells; Q2 quadrant represents the percentage of late apoptotic cells; Q3 quadrant represents the percentage of live cells and Q4 quadrant represents the percentage of early apoptotic cells. **B)** Flow cytometric analysis of apoptotic index in different groups.The values are expressed as mean ± SD of n = 6 observations from each group. $^{**}p < 0.01$ and $^{*}p < 0.05$ w.r.t. control, $^{\#\#\#}p < 0.001$, $^{\#\#}p < 0.01$ and $^{\#}p < 0.05$ w.r.t. DMSO only and $^{\$\$\$}p < 0.001$ w.r.t. DMH + DSS group.

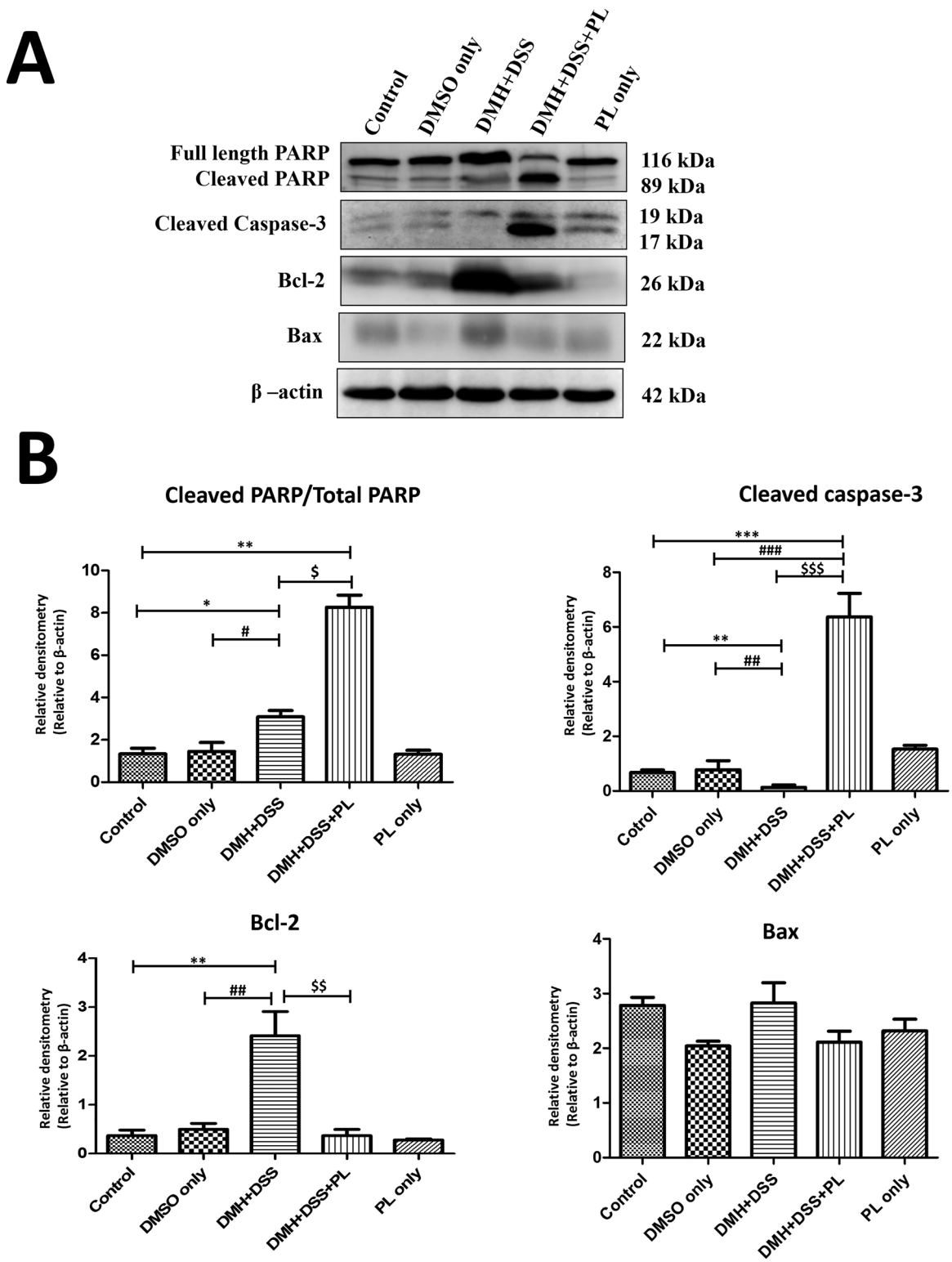

Fig. 8. Effect of PL on marker proteins of apoptosis using western blotting. **A)** Representative immunoblots for PARP 1/2, cleaved caspase-3, Bcl-2 and Bax. β-actin was used as internal control. **B)** Densitometric analysis for cleaved PARP/Total PARP, cleaved caspase-3, Bcl-2 and Bax assessed by AlphaView software. The data were observed for n = 4 animals/group.The values are expressed as mean ± SD of n = 4 observations from each group. $^{***}p < 0.001$ w.r.t. control, $^{*}p < 0.05$ w.r.t. control, $^{\#\#\#}p < 0.001$ w.r.t. DMSO only, $^{\$}p < 0.05$ w.r.t. DMH + DSS and $^{\$\$\$}p < 0.001$ w.r.t. DMH + DSS group.

groups. However, PL administration to DMH + DSS treated animals led to a significant increase in apoptotic index in these animals as compared to DMH + DSS treated animals.

As demonstrated earlier, PL administration induced apoptotic cell death in DMH + DSS treated animals. In view of the fact that activation of caspases and PARP cleavage are hallmarks of apoptosis, we next investigated the key regulatory proteins involved in apoptosis such as active caspase -3 and its downstream target PARP as well as Bcl-2 family proteins by western blotting (Fig. 8). The data shown here clearly depicts a diminished activity of caspase -3 in DMH + DSS treated

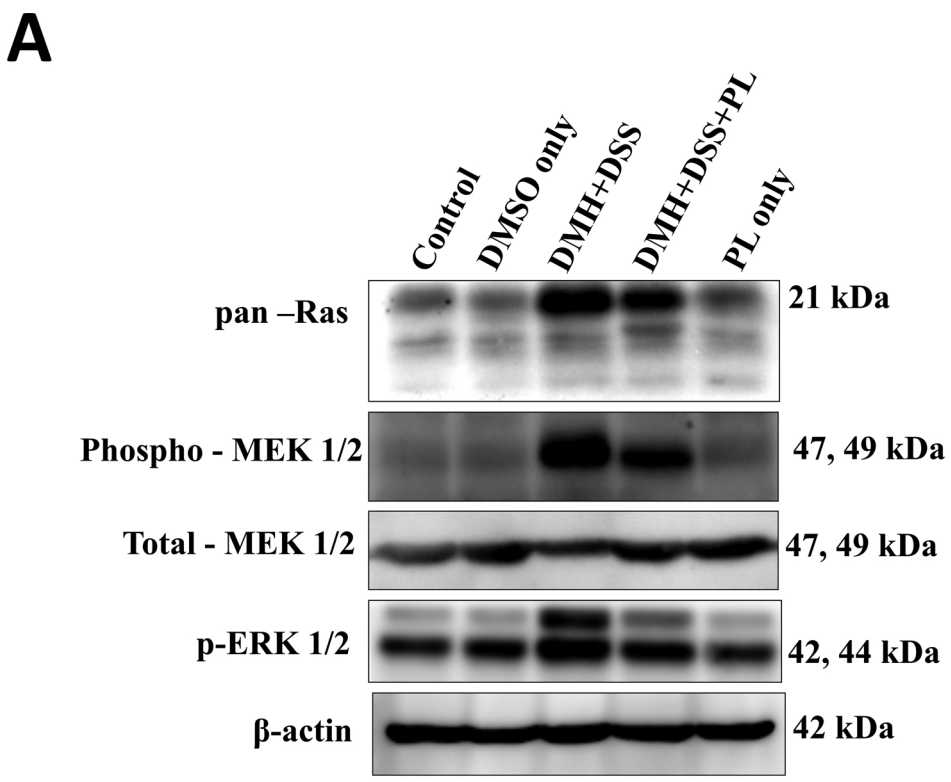

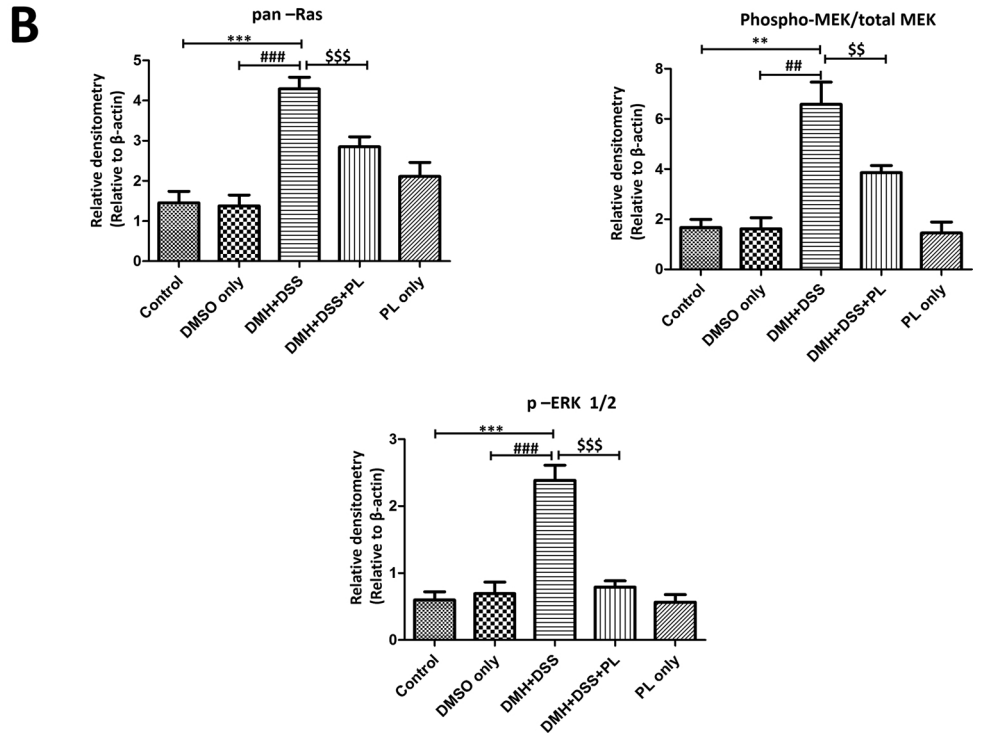

Fig. 9. Effect of PL on Ras signaling pathway using western blotting. **A)** Representative immumoblots for Ras, Phospho -MEK1/2, Total MEK1/2 and Phospho -ERK1/2. β-actin was used as internal control. **B)** Densitometric analysis for Ras, activated MEK1/2 and phospho-ERK1/2 assessed by AlphaView software. The data were observed for n = 4 animals/group. The values are expressed as mean ± SD of n = 4 observations from each group. ***$p < 0.001$, **$p < 0.01$ and *$p < 0.05$ w.r.t. control, $^{###}p < 0.001$, $^{##}p < 0.01$ and $^{#}p < 0.05$ w.r.t. DMSO only and $^{\$\$\$}p < 0.001$, $^{\$\$}p < 0.01$ and $^{\$}p < 0.005$ w.r.t. DMH + DSS group.

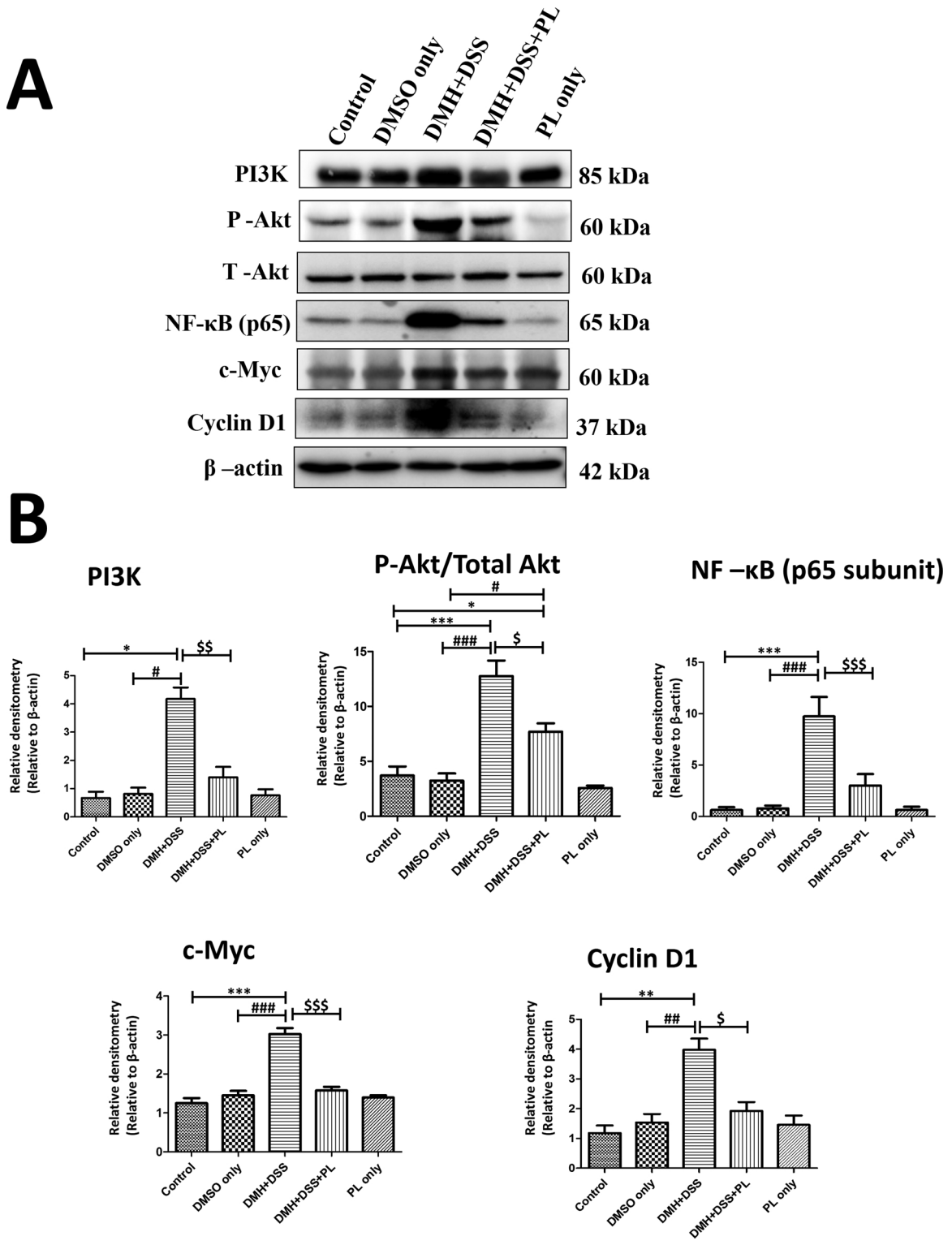

Fig. 10. Effect of PL on marker proteins involved in cell proliferation using western blotting. **A)** Representative immumoblots for PI3K, Phospho-Akt/Total Akt, NF-κB (p65 subunit), c-Myc and cyclin D1. β-actin was used as internal control. **B)** Densitometric analysis for PI3K, Phospho-Akt/Total Akt, NF-κB (p65 subunit), c-Myc and cyclin D1assessed by AlphaView software. The data were observed for n = 4 animals/group. The values are expressed as mean ± SD of n = 4 observations from each group. $^{***}p < 0.001$, $^{**}p < 0.01$ and $^{*}p < 0.05$ w.r.t. control, $^{###}p < 0.001$, $^{##}p < 0.01$ and $^{#}p < 0.05$ w.r.t. DMSO only and $^{\$\$\$}p < 0.001$, $^{\$\$}p < 0.01$ and $^{\$}p < 0.005$ w.r.t. DMH + DSS group.

animals as evident from a decrease in the expression of cleaved caspase 3 fragments (Fig. 8 B). The reduced activity of caspase-3 is suggestive of reduced apoptosis that sets a stage for cancer establishment in colon tissue. The treatment of DMH + DSS animals with PL significantly increased the expression of both fragments of active caspase -3 which demonstrates that the induced apoptosis by PL is mediated *via* activation of caspase-3. It is a well known fact that active caspase -3 cleaves PARP into two fragments with molecular weight 116 and 89 kDa. As expected, there was an abrogation in PARP cleavage in protein samples isolated from DMH + DSS treated animals (Fig. 8 B). PL administration,

however, resulted in significant accumulation of cleaved PARP in DMH + DSS + PL group.

Bcl-2 family proteins specifically Bax (pro-apoptotic) and Bcl-2 (anti-apoptotic) play key role in regulating mitochondria mediated apoptosis. Therefore, levels of these two major proteins were also analyzed to determine whether PL induces apoptosis through intrinsic/mitochondrial pathway in the current study. DMH + DSS treatment led to a significant increase in the levels of Bcl-2 proteins as compared to control and DMSO only treated animals (Fig. 8 B). On the other hand, the levels of Bcl-2 were significantly reduced in DMH + DSS + PL group suggesting the ability of PL to drive the cancer cells towards apoptosis. There was no significant change in the levels of Bcl-2 in PL only treated animals as compared to control and DMSO only treated animals. The levels of Bax were also analyzed but no significant alteration in its expression was observed in any of the groups (Fig. 8 B).

3.6. Effect of PL on Ras/PI3K/Akt/mTOR signaling pathway

To uncover the molecular mechanism underlying PL induced apoptosis, we next examined the effect of PL on Ras and PI3K/Akt/mTOR signaling pathway by assessing the key proteins of these pathways (Figs. 9 and 10). Oncogenic activation of Ras protein owing to missense mutation is a well known marker of incessant tumor cell proliferation. Western blot analysis revealed that the treatment with DMH + DSS led to a significant increase in the levels of Ras proteins as compared to control and DMSO only treated group animals (Fig. 9 B). Conversely, the levels of Ras proteins were significantly reduced in DMH + DSS + PL animals suggesting the antiproliferative nature of PL. Activated Ras protein targets MEK to trigger ERK phosphorylation and its nuclear translocation for expression of genes involved in cell proliferation. Therefore, we further investigated these downstream targets. The results revealed that there was a significant increase in the levels of activated MEK1/2 and phospho-ERK1/2 in DMH + DSS treated animals as compared to control animals. However, the levels of both phosphorylated MEK1/2 and phospho-ERK1/2 were decreased in DMH + DSS + PL treated animals corroborating our data on inhibition of Ras signaling pathway by PL for inhibition in tumor cell growth and proliferation (Fig. 9 B). There was no significant alteration in PL only treated animals as compared to control and vehicle treated group.

Ras oncoprotein also interacts with PI3K and triggers Akt phosphorylation and its subsequent activation. Therefore, we next examined PI3K levels and Ser473 phosphorylation of Akt, which measures both Akt/ mTORC1 and mTORC2 activity (Fig. 10B). Treatment of animals with DMH + DSS showed a significant increase in the levels of both PI3K and phosphorylated Akt as compared to control and DMSO treated animals. However, there was a significant reduction in the levels of PI3K and phosphorylated Akt in DMH + DSS + PL animals. We also checked the expression of downstream effector of Akt i.e. NF-κB, a transcription factor known for providing resistance to apoptosis by upregulating expression of anti-apoptotic proteins such as Bcl-2. In the present study, we observed a significant increase in the expression of NF-κB in DMH + DSS treated animals as compared to control animals (Fig. 10B). The enhanced expression of NF-κB can be ascribed to chronic inflammation ensued by cyclic treatment with inflammatory agent DSS. However, a significant decrease in NF-κB was noticed in DMH + DSS + PL treated animals as compared to DMH + DSS treated animals. There was no significant alteration in the basal level of NF-κB expression in vehicle treated groups as compared to control group.

Ras proteins can induce spontaneous activation of c-Myc [26–28], anoncogenic transcription factor that upregulates key proteins of cell cycle machinery and drive oncogenic cell proliferation [29,30]. In the present study, it was observed that c-Myc levels were significantly increased in DMH + DSS treated animals as compared to control and DMSO treated animals (Fig. 10B). On the other hand, a marked decrease in the levels of c-Myc was seen in DMH + DSS + PL treated animals. There was no significant alteration in the basal c-Myc level in any of the control groups. c-Myc is reported to control the cell cycle machinery by regulating the levels of various cyclins. Further evaluation of cyclin D1 levels in tissue samples exhibited a significant increase in its levels in DMH + DSS treated animals as compared to control groups which corroborates with our results for cell proliferation markers (Fig. 10B). Contrary to this, cyclin D1 levels were significantly reduced in DMH + DSS + PL treated animals further strengthening the cytostatic nature of PL.

3.7. Effect of PL on toxicity profile

To the best of our knowledge, we have evaluated PL for its chemopreventive potential in CRC animal model for the first time. Therefore, it was necessary to examine whether PL is toxic to the animals. In view of this, we analyzed the serum levels of AST, ALT, urea and creatinine for the assessment of liver and kidney function respectively. Treatment with DMH + DSS led to a significant increase in AST and ALT levels as well as those of urea and creatinine levels as compared to control animals (Fig. 11 B). On the other hand, a marked decrease in the levels of these enzymes was observed in DMH + DSS + PL treated animals suggesting that PL helps to reduce the toxicity caused due to the treatment of DMH + DSS. In comparison to control animals, we did observe a slight but a non significant increase in ALT values in case of PL only treated animals. Further examination of liver sections did not reveal any significant alterations as compared to control animals which further confirm that PL administration does not cause any hepatotoxicity or nephrotoxicity (Fig. 11 A).

4. Discussion

Chemoprevention is gaining attention worldwide due to the use of natural and safe agents with no adverse side effects [31]. A comprehensive look at the epidemiology of CRC clearly highlights that its incidence in regions such as Indian subcontinents is among the lowest in the world. This can be ascribed to differences in diet, environment and routine lifestyle. A specialty of Indian diet is the routine use of spices in Indian cuisine for flavor enhancement. In addition, use of spices in medicinal formulations is an age old practice in Ayurveda, Unani and Siddha medicine. Evidence from pre-clinical and clinical studies indicates that spices prevent CRC by modulating different pathways involved in tumorigenesis [32]. After curcumin, another spice which is gaining considerable attention for its anticancer activity is PL, a principle bioactive compound present in long pepper, a common Indian dietary spice [33]. Recently, PL has been reported to inhibit cancer cell proliferation and tumor growth in various *in vitro* studies [10]. However, till date, no study has been conducted to evaluate PL for its chemopreventive/chemotherapeutic potential in CRC animal model. Therefore, the present study was designed to evaluate the chemopreventive potential of PL in DMH/DSS induced colorectal cancer which closely mimics adenoma–carcinoma sequence of human CRC.

The first noticeable change observed in cancer patients is loss of weight and appetite as the disease progresses and is termed as cancer cachexia. Similarly, reduction in food intake and average gain in body weight are characteristic feature of AOM/DSS induced CRC in mice [34]. In the current study, a significant decline in food intake was observed during 2nd and 3rd DSS exposure cycle (5th and 8th week). This may be related to the presence of DSS in drinking water. DMH/DSS exposure has been reported to cause intestinal damage ensuing inflammatory conditions which in turn results in reduced food intake. The reduction in food intake and body weight in DMH + DSS treated animals might be linked to tumor progression in these animals. The significant improvement in food intake and gain in average body weight in DMH + DSS + PL treated animals can be attributed to anti-inflammatory property of PL that might have inhibited intestinal inflammation caused by DMH + DSS treatment.

The gross and histopathological examination of colon tissue sections

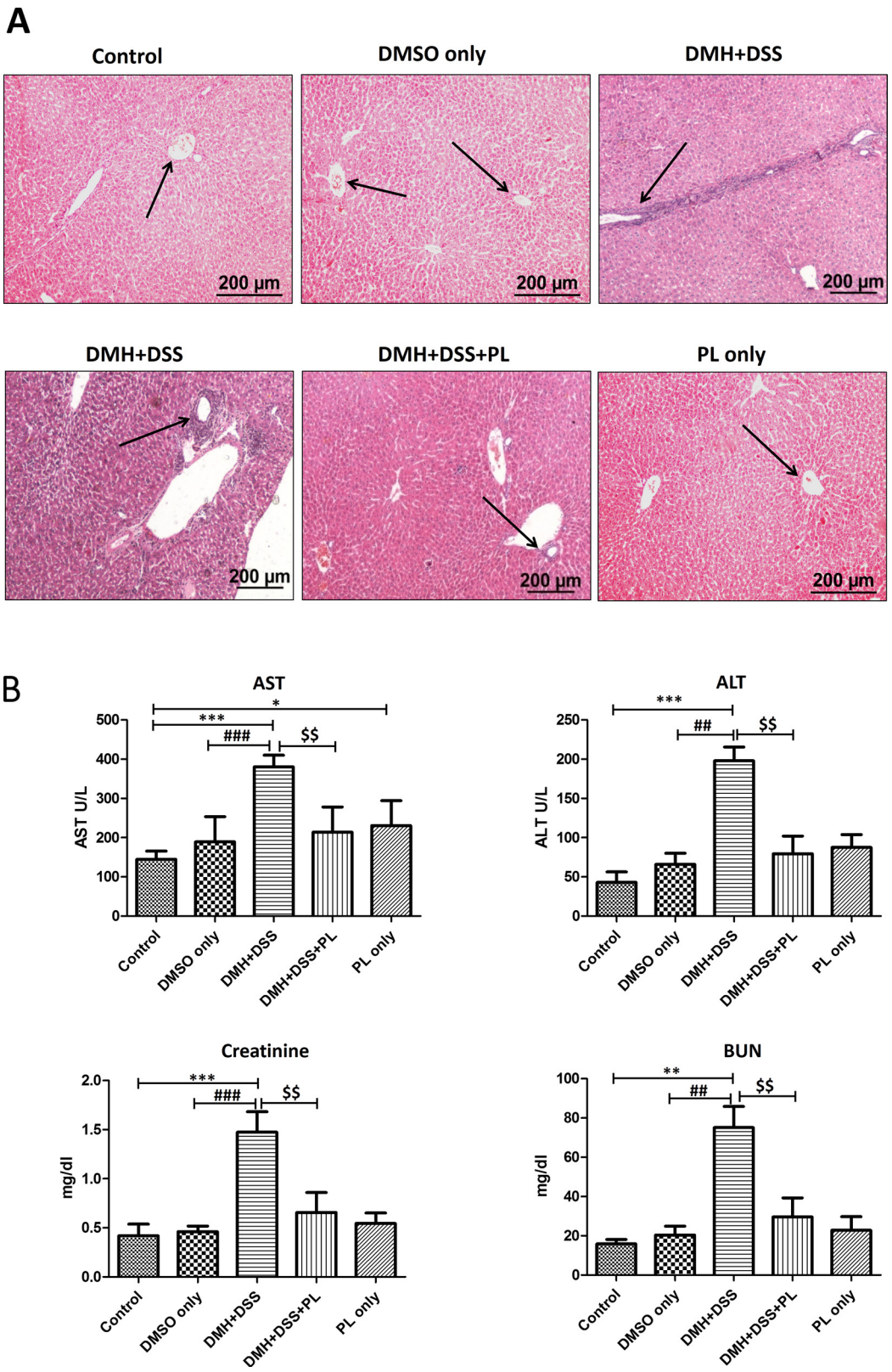

Fig. 11. A) Representative images of H & E stained liver sections. Control and DMSO only group showing normal morphology of liver, DMH + DSS treated group showing increased portal tract inflammation (arrow), DMH + DSS + PL treated group showing normal liver tissue histology with no sign of portal tract inflammation (arrow) and PL only group. The images were taken at 10 × . **B)** is representative histograms showing effect of PL on liver and kidney function tests. The values are expressed as mean ± SD of n = 4 observations from each group. ***$p < 0.001$, **$p < 0.01$ and *$p < 0.05$ w.r.t. control, $^{###}p < 0.001$, $^{##}p < 0.01$ and $^{\$\$}p < 0.01$ w.r.t. DMH + DSS group.

of control and DMSO treated mice showed no sign of abnormality in crypt morphology while mice treated with DMH + DSS developed multiple tumor nodules and thus an increase in tumor burden and volume. Histopathological examination revealed the presence of multiple malignant lesions such as polyploid adenoma, hyperplasia and cancer *in situ* which confirm the establishment of colon cancer in these animals. Similar observations in the same model have also been reported earlier [8]. Interestingly, PL treatment to DMH + DSS exposed animals significantly reduced the tumor burden and volume. In addition, histopathological evaluation revealed that PL treatment reduced the neoplastic regions such as dysplasia and cancer *in situ* in colon sections. Overall, these observations suggest that PL inhibits DMH + DSS induced tumor development in the colon and thus exhibits antitumor effect. Till date, there is no *in vivo* study available on the chemopreventive effect of PL on tumor growth in CRC, particularly in DMH/DSS model.

Apoptosis is a programmed cell death that eliminates damaged and aged cells from the body under normal physiological conditions [35]. Evasion from apoptosis is one of the key hallmarks of cancer cells during their malignant transformation. Understanding the underlying mechanism of programmed cell death is the primary criterion for developing anticancer therapeutic strategies. Many natural agents such as curcumin, resveratrol, and lycopene have been documented to modulate apoptotic pathway and thereby act as anticancer agents [5]. In the present study, the effect of PL on apoptotic pathway was assessed through multiple approaches: morphological evaluation (Hoechst 33,342/PI staining), surface marker (Annexin V/PI staining) and effector proteins (caspase-3 and PARP cleavage). Transformation of normal cell to neoplastic one is generally preceded by resistance to apoptosis and thereby a net decrease in apoptotic index. We also observed a significant decrease in the apoptotic index in DMH + DSS treated animals as evident from a decrease in propidium iodide staining, annexin V expression, caspase-3 and PARP activity. An evident and highly significant increase in the apoptotic index was observed in DMH + DSS + PL group. An increase in the caspase-3 activity can be documented by the presence of its cleaved fragments of molecular weight 17 and 19 kDa. In the present study, we observed a significant inhibition of active caspase-3 levels in DMH + DSS treated animals as compared to control groups, an indication of reduced apoptosis in this group. Conversely, treatment with PL to DMH + DSS treated animals resulted in a significant increase in the levels of active caspase-3 fragments, suggestive of increased apoptosis in these animals. PARP is an important enzyme to maintain genomic integrity in response to DNA damage. It is well established fact that active caspase-3 cleaves its downstream target PARP into two fragments of molecular weight 116 and 89 kDa in DNA damage induced apoptosis in a variety of cells [36]. In fact, a significant increase in PARP cleavage was observed in DMH + DSS + PL treated animals. These results are in accordance to the previous *in vitro* reports in which PL induced caspase mediated apoptosis [22].

Regulatory proteins of intrinsic apoptotic pathway in cancer are Bcl-2 family which include both pro-apoptotic (*e.g.* Bax, Bad and Bak) and anti-apoptotic proteins (*e.g.* Bcl-2, Bcl-xL, Bcl-w and Mcl-1) [37].The interplay between these proteins is a determining factor for the release of cytochrome *c* from mitochondria and ensuing apoptosis. Further, evidence for the major role of Bcl-2 and its family members is provided by the fact that overexpression of Bcl-2 protein has been reported in various human cancers and is also an indication of reduction in survival time and drug resistance [38]. To further delineate the mechanism of action of PL to induce apoptosis, we analyzed the expression of Bax and Bcl-2. As expected, treatment with DMH + DSS resulted in a significant increase in Bcl-2 levels, however, Bax levels were not significantly altered which points towards the major role played by Bcl-2 protein in cancer progression. A significant decrease in Bcl-2 levels was noticed on treatment with PL. A Bax/Bcl-2 ratio is more important as a determinant of apoptosis. Even if we did not observe any alteration in Bax levels, a net increase in Bax/Bcl-2 ratio would result in apoptosis. These results exhibited a close reflection of *in vitro* anticancer studies of PL done by other research group which also showed an involvement of apoptotic mitochondrial pathway in response to PL [39].

Uncontrolled cell growth and proliferation is a characteristic feature of most of the cancers. Constitutive activation of Ras proteins due to missense mutations particularly in K-Ras is frequently observed in human CRC [40]. Activated Ras stimulates cellular proliferation by modulating a wide array of intracellular effector pathways which ultimately converge to promote pro-growth and to inhibit antigrowth signals in transformed cell. The activation of Ras signaling pathway was observed in this study on treatment with DMH + DSS which points towards increased cell proliferation and levels of anti-apoptotic entities in the colon of these animals. Further, enhanced levels of its downstream target proteins such as phosphorylated MEK and ERK supported the notion that DMH + DSS treatment activated Ras signaling for tumor establishment. However, the decreased levels of Ras and its associated downstream targets suggested the involvement of this pathway in the chemopreventive action of PL.

Moreover, Ras mediated proliferative signals have also been reported to upregulate several transcription factors that are crucial for cell cycle checkpoints. An important transcription factor in this category is c-myc that controls cell cycle machinery and triggers the expression of G1 cyclins, especially cyclin D types [30]. In the current study, DMH + DSS treatment led to a significant increase in the expression of Ras protein and c-myc that indicates high rate of tumor cell proliferation in these animals. In addition, we also observed a significant increase in the levels of cyclin D1, a downstream target of c-myc which further supported our hypothesis of activation of Ras signalling pathway. Conversely, downregulation of Ras proteins, c-myc and cyclin D1 on treatment with PL to DMH + DSS group suggested the antiproliferative nature of PL towards tumor cells. Furthermore, cell cycle arrest at G2/M phase on PL administration also proved the antineoplastic potential of PL. These observations are in accordance with other *in vitro* studies reporting G2/M arrest [20], inhibition of cyclin D1 and c-myc expression [14] on treatment with PL. Ras protein interacts with PI3K that eventually results in phosphorylation and activation of Akt. Phosphorylated Akt is a well-established cell survival factor because it upregulates expression of antiapototic Bcl-2 protein [41]. In the present study DMH + DSS treatment also led to a significant increase in the levels of phosphorylated Akt and subsequently Bcl-2 proteins. On the other hand, PL treatment to DMH + DSS treated animals led to a significant reduction in the levels phosphorylated Akt as well as Bcl-2 which strongly indicates antineoplastic activity of PL. The results of present study are in concurrence with an earlier study where PL has been shown to promote cell death in prostate and breast cancer cell lines by inhibiting Akt phosphorylation [18]. The activated Akt stimulates IKK activity that eventually results in activation of NF-κB transcription factor [42,43]. In the present study, we further investigated the effect of PL on the major cell surivival pathway i.e. Akt/NF-κB pathway. We observed a significant increase in the levels of NF-κB in DMH + DSS treated animals. The increased NF-κB expression can be ascribed to consequence of Akt activation. However, on PL treatment we observed a significant decrease in the levels of NF-κB that could be explained by the anti-inflammatory activity of PL. The data shown here has demonstrated that PL mitigated Ras protein levels which subsequently repressed the downstream signalling cascade hub Akt/NF-κB.

It is mandatory to determine the toxic potential of any agent to be administered *in vivo*. In addition, carcinogen treatment such as DMH has been reported to cause hepatotoxicity and nephrotoxicity [44]. Therefore, analysis of serum biochemical parameters pertaining to liver and kidney function *i.e.* AST, ALT, urea and creatinine respectively were investigated in the present study. DMH is metabolized in the liver to methylazoxy methanol and transformed to carcinogenic moiety *i.e.* methyldiazonium [45]. The function of kidney is to maintain the optimum chemical composition of the body fluids by acidification of urine

and removal of metabolite wastes as urea, uric acid, creatinine and ions. An increase in the concentrations of these metabolites in blood has been observed during cancer progression. The cyclic treatment with DSS hastens the progression of colorectal cancer and thus DMH induced hepatic and renal toxicity. Treatment with DMH + DSS led to a significant elevation in the serum levels of AST, ALT, urea and creatinine in comparison to respective control groups. Similar results have also been previously reported in the same animal model from our lab [34]. However, PL treatment to DMH + DSS exposed animals led to a significant reduction in the levels of serum marker enzymes like AST and ALT as well as blood urea and creatinine suggesting its protective effect against carcinogen mediated organ toxicity and damage. We also observed that PL drug itself did not have any significant toxicity as no significant alteration was observed in the biochemical values of PL only treated animals in the present study.

To conclude, the present study demonstrated that PL exerted a potent chemopreventive effect in DMH + DSS induced experimental colon carcinogenesis. Our study emphasizes that PL inhibits tumor growth by targeting multiple components of Ras/PI3K/Akt signaling axis and its downstream events such as activation of NF-κB and evasion from apoptosis. Therefore, PL appears to be an attractive bioactive phytochemical with future clinical application for colon cancer treatment.

Conflict of interest

The authors declare no conflict of interest.

Acknowledgement

SK thanks University Grants Commission (UGC), New Delhi for providing Senior Research Fellowship to carry out the research work. The authors acknowledge the assistance from University Grants Commission and Department of Science & Technology as the department is supported under UGC SAP and DST-PURSE program.

References

[1] M. Arnold, M.S. Sierra, M. Laversanne, I. Soerjomataram, A. Jemal, F. Bray, Global patterns and trends in colorectal cancer incidence and mortality, Gut (2016) 1–9.
[2] C.J.A. Punt, M. Koopman, L. Vermeulen, From tumour heterogeneity to advances in precision treatment of colorectal cancer, Nat. Rev. Clin. Oncol. 14 (2016) 235–246.
[3] A. Polk, K. Vistisen, M. Vaage-Nilsen, D.L. Nielsen, A systematic review of the pathophysiology of 5-fluorouracil-induced cardiotoxicity, BMC Pharmacol. Toxicol. 15 (2014) 47.
[4] A.M. Fajardo, G.A. Piazza, Chemoprevention in gastrointestinal physiology and disease. Anti-inflammatory approaches for colorectal cancer chemoprevention, Am. J. Physiol.,Gastrointest. Liver Physiol. 309 (2015) G59–G70.
[5] R. Kotecha, A. Takami, J.L. Espinoza, Dietary phytochemicals and cancer chemoprevention: a review of the clinical evidence, Oncotarget (2016) 52517–52529.
[6] A.L. Harvey, R. Edrada-Ebel, R.J. Quinn, The re-emergence of natural products for drug discovery in the genomics era, Nat. Rev. Drug Discov. 14 (2015) 111–129.
[7] V. Fazio, M. Robertis, E. Massi, M. Poeta, S. Carotti, S. Morini, L. Cecchetelli, E. Signori, The AOM/DSS murine model for the study of colon carcinogenesis: from pathways to diagnosis and therapy studies, J. Carcinog. 10 (2011) 1–20.
[8] T. Tanaka, Development of an inflammation-associated colorectal cancer model and its application for research on carcinogenesis and chemoprevention, Int. J. Inflam. 2012 (2012) 1–17.
[9] J. Zheng, Y. Zhou, Y. Li, D.P. Xu, S. Li, H. Bin Li, Spices for prevention and treatment of cancers, Nutrients 8 (2016) 1–35.
[10] L. Raj, T. Ide, A.U. Gurkar, M. Foley, M. Schenone, X. Li, N.J. Tolliday, T.R. Golub, S. a Carr, A.F. Shamji, A.M. Stern, A. Mandinova, S.L. Schreiber, S.W. Lee, Selective killing of cancer cells by a small molecule targeting the stress response to ROS, Nature 475 (2011) 231–234.
[11] H.O. Jin, Y.H. Lee, J.A. Park, H.N. Lee, J.H. Kim, J.Y. Kim, B.R. Kim, S.E. Hong, H.A. Kim, E.K. Kim, W.C. Noh, J. Il Kim, Y.H. Chang, S. Il Hong, Y.J. Hong, I.C. Park, J.K. Lee, Piperlongumine induces cell death through ROS-mediated CHOP activation and potentiates TRAIL-induced cell death in breast cancer cells, J. Cancer Res. Clin. Oncol. 140 (2014) 2039–2046.
[12] S.S. Han, V.S. Tompkins, D.J. Son, N.L. Kamberos, L.L. Stunz, A. Halwani, G.A. Bishop, S. Janz, Piperlongumine inhibits LMP1/MYC-dependent mouse B-lymphoma cells, Biochem. Biophys. Res. Commun. 436 (2013) 660–665.
[13] J. Ryu, M.-J. Kim, T.-O. Kim, T.-L. Huh, S.-E. Lee, Piperlongumine as a potential activator of AMP-activated protein kinase in HepG2 cells, Nat. Prod. Res. 28 (2014) 2040–2043.
[14] J.G. Han, S.C. Gupta, S. Prasad, B.B. Aggarwal, Piperlongumine chemosensitizes tumor cells through interaction with cysteine 179 of IκBα kinase, leading to suppression of NF-κB-regulated gene products, Mol. Cancer Ther. 13 (2014) 2422–2435.
[15] J. Zheng, D.J. Son, S.M. Gu, J.R. Woo, Y.W. Ham, H.P. Lee, W.J. Kim, J.K. Jung, J.T. Hong, Piperlongumine inhibits lung tumor growth via inhibition of nuclear factor kappa B signaling pathway, Sci. Rep. 6 (2016) 1–13.
[16] H. Randhawa, K. Kibble, H. Zeng, M.P. Moyer, K.M. Reindl, Activation of ERK signaling and induction of colon cancer cell death by piperlongumine, Toxicol. In Vitro 27 (2013) 1626–1633.
[17] Y. Wang, J.-W. Wang, X. Xiao, Y. Shan, B. Xue, G. Jiang, Q. He, J. Chen, H.-G. Xu, R.-X. Zhao, K.D. Werle, R. Cui, J. Liang, Y.-L. Li, Z.-X. Xu, Piperlongumine induces autophagy by targeting p38 signaling, Cell Death Dis. 4 (2013) 1–11.
[18] P. Makhov, K. Golovine, E. Teper, A. Kutikov, R. Mehrazin, A. Corcoran, A. Tulin, R.G. Uzzo, V.M. Kolenko, Piperlongumine promotes autophagy via inhibition of Akt/mTOR signalling and mediates cancer cell death, Br. J. Cancer 110 (2014) 899–907.
[19] X.-X. Xiong, J.-M. Liu, X.-Y. Qiu, F. Pan, S.-B. Yu, X.-Q. Chen, Piperlongumine induces apoptotic and autophagic death of the primary myeloid leukemia cells from patients via activation of ROS-p38/JNK pathways, Acta Pharmacol. Sin. 36 (2015) 362–374.
[20] C. Duan, B. Zhang, C. Deng, Y. Cao, F. Zhou, L. Wu, M. Chen, S. Shen, G. Xu, S. Zhang, G. Duan, H. Yan, X. Zou, Piperlongumine induces gastric cancer cell apoptosis and G2/M cell cycle arrest both *in vitro* and *in vivo*, Tumor Biol. 37 (2016) 10793–10804.
[21] F. Wang, Y. Mao, Q. You, D. Hua, D. Cai, Piperlongumine induces apoptosis and autophagy in human lung cancer cells through inhibition of PI3K/Akt/mTOR pathway, Int. J. Immunopathol. Pharmacol. 28 (2015) 362–373.
[22] S. Shrivastava, P. Kulkarni, D. Thummuri, M.K. Jeengar, V.G.M. Naidu, M. Alvala, G.B. Redddy, S. Ramakrishna, Piperlongumine, an alkaloid causes inhibition of PI3K/Akt/mTOR signaling axis to induce caspase-dependent apoptosis in human triple-negative breast cancer cells, Apoptosis 19 (2014) 1148–1164.
[23] L.M. Sanders, C.E. Henderson, M.Y. Hong, R. Barhoumi, R.C. Burghardt, N. Wang, C.M. Spinka, R.J. Carroll, N.D. Turner, R.S. Chapkin, J.R. Lupton, An increase in reactive oxygen species by dietary fish oil coupled with the attenuation of antioxidant defenses by dietary pectin enhances rat colonocyte apoptosis, J. Nutr. 134 (2004) 3233–3238.
[24] R.I. Freshney, Culture of Animal Cells: A Manual of Basic Technique and Specialized Applications, sixth edition, (2011).
[25] W. Xia, S. Spector, L. Hardy, S. Zhao, A. Saluk, L. Alemane, N.L. Spector, Tumor selective G2/M cell cycle arrest and apoptosis of epithelial and hematological malignancies by BBL22, a benzazepine, Proc. Natl. Acad. Sci. 97 (2000) 7494–7499.
[26] W. Kruszewski, R. Kowara, R. Rzepko, C. Warezak, J. Zielinski, G. Gryglewski, A. Kopacz, T. Jastrzebski, T. Pawelczyk, K-RAS point mutation, and amplification of C-MYC and C-ERBB2 in colon adenocarcinoma, Folia Histochem. Cytobiol. 42 (2004) 173–179.
[27] Y. Pylayeva-Gupta, E. Grabocka, D. Bar-Sagi, RAS oncogenes: weaving a tumorigenic web, Nat. Rev. Cancer 11 (2011) 761–774.
[28] R. Sears, F. Nuckolls, E. Haura, Y. Taya, K. Tamai, J.R. Nevins, Multiple Ras-dependent phosphorylation pathways regulate Myc protein stability, Genes Dev. 14 (2000) 2501–2514.
[29] C.V. Dang, MYC on the path to cancer, Cell 149 (2012) 22–35.
[30] Q. Yu, M.A. Ciemerych, P. Sicinski, Ras and Myc can drive oncogenic cell proliferation through individual D-cyclins, Oncogene 24 (2005) 7114–7119.
[31] A.K. Greiner, R.V. Papineni, S. Umar, Chemoprevention in gastrointestinal physiology and disease. Natural products and microbiome, Am. J. Physiol. Gastrointest. Liver Physiol. 307 (2014) G1–15.
[32] B. Aggarwal, S. Prasad, B. Sung, S. Krishnan, S. Guha, Prevention and treatment of colorectal cancer by natural agents from mother nature, Curr. Colorectal Cancer Rep. 9 (2013) 37–56.
[33] D.P. Bezerra, C. Pessoa, M.O. De Moraes, N. Saker-Neto, E.R. Silveira, L.V. Costa-Lotufo, Overview of the therapeutic potential of piplartine (piperlongumine), Eur. J. Pharm. Sci. 48 (2013) 453–463.
[34] I. Rani, K. Vaiphei, N. Agnihotri, Supplementation of fish oil augments efficacy and attenuates toxicity of 5-fluorouracil in 1,2-dimethylhydrazine dihydrochloride/dextran sulfate sodium-induced colon carcinogenesis, Cancer Chemother. Pharmacol. 74 (2014) 309–322.
[35] S. Baig, I. Seevasant, J. Mohamad, A. Mukheem, H.Z. Huri, T. Kamarul Potential of apoptotic pathway-targeted cancer therapeutic research: where do we stand? Cell Death Dis. 7 (2016) 1–11.
[36] A.H. Boulares, A.G. Yakovlev, V. Ivanova, B.A. Stoica, G. Wang, S. Iyer, M. Smulson, Role of poly(ADP-ribose) polymerase (PARP) cleavage in apoptosis. Caspase 3-resistant PARP mutant increases rates of apoptosis in transfected cells, J. Biol. Chem. 274 (1999) 22932–22940.
[37] M. Kvansakul, M.G. Hinds, The Bcl-2 family: Structures, interactions and targets for drug discovery, Apoptosis. 20 (2015) 136–150.
[38] J. Skommer, T. Brittain, S. Raychaudhuri, Bcl-2 inhibits apoptosis by increasing the time-to-death and intrinsic cell-to-cell variations in the mitochondrial pathway of cell death, Apoptosis 15 (2010) 1223–1233.
[39] S.-Y. Chen, G.-H. Liu, W.-Y. Chao, C.-S. Shi, C.-Y. Lin, Y.-P. Lim, C.-H. Lu, P.-Y. Lai, H.-R. Chen, Y.-R. Lee, Piperlongumine suppresses proliferation of human oral squamous cell carcinoma through cell cycle arrest, apoptosis and senescence, Int. J. Mol. Sci. 17 (2016) 1–14.
[40] A.I. Phipps, D.D. Buchanan, K.W. Makar, A.K. Win, J.A. Baron, N.M. Lindor, J.D. Potter, P.A. Newcomb KRAS-mutation status in relation to colorectal cancer survival: the joint impact of correlated tumour markers, Br. J. Cancer 108 (2013)

1757–1764.
[41] S. Pugazhenthit, A. Nesterova, C. Sable, K.A. Heidenreich, L.M. Boxer, L.E. Heasley, J.E.B. Reusch, Akt/protein kinase B up-regulates Bcl-2 expression through cAMP-response element-binding protein, J. Biol. Chem. 275 (2000) 10761–10766.
[42] O.N. Ozes, L.D. Mayo, J. a Gustin, S.R. Pfeffer, L.M. Pfeffer, D.B. Donner, NF-kappaB activation by tumour necrosis factor requires the Akt serine-threonine kinase, Nature 401 (1999) 82–85.
[43] D. Bai, L. Ueno, P.K. Vogt, Akt-mediated regulation of NFκB and the essentialness of NFκB for the oncogenicity of PI3K and Akt, Int. J. Cancer 125 (2009) 2863–2870.
[44] G. Brambilla, M. Cavanna, S. Parodi, L. Sciaba, A. Pino, L. Robbiano, DNA damage in liver, colon, stomach, lung and kidney of BALB/c mice treated with 1,2-dimethylhydrazine, Int. J. Cancer 22 (1978) 174–180.
[45] W.M. Castleden, K.B. Shilkin, Diet, liver function and dimethylhydrazine-induced gastrointestinal tumours in male Wistar rats, Br. J. Cancer 39 (1979) 731–739.